10 Flexibility Analyses and Their Applications in Solar-Driven Membrane Distillation Desalination System Designs

Vincentius Surya Kurnia Adi and Chuei-Tin Chang

CONTENTS

Owing to the rapidly growing world population and the alarming effects of global warming, there appears to be an ever-increasing demand for freshwater almost everywhere. For this reason, considerable effort has been devoted in recent years to develop an efficient and sustainable desalination technology. Among various alternatives, the *air gap membrane distillation* (AGMD) is widely considered as a promising candidate since the energy consumed per unit of water generated by this method is the lowest (Cabassud and Wirth, 2003; Ben Bacha et al., 2007; Bui et al., 2010). Many researchers have already constructed rigorous mathematical models to simulate and analyze the underlying transport phenomena so as to identify the key variables affecting the water flux in an AGMD module (Koschikowski et al., 2003; Meindersma et al., 2006; Ben Bacha et al., 2007; Chang et al., 2010). Particularly, Ben Bacha et al. (2007) and Chang et al. (2010, 2012) have built models of all units embedded in a *solar-driven membrane distillation desalination system* (SMDDS), that is, (1) the solar absorber, (2) the thermal storage tank, (3) the counter-flow shell-and-tube heat exchanger, (4) the AGMD modules, and (5) the distillate tank, and then discussed various operational and control issues accordingly. The process flow diagram of a typical SMDDS design can be found in Figure 10.1. Gálvez et al. (2009) meanwhile, designed a 50 m^3/day desalination setup with an innovative solar-powered membrane, and Guillen-Burrieza et al. (2011) also assembled a solar-driven AGMD pilot plant. These two studies were performed with the common goal of minimizing energy consumption per unit of distillate produced. Note that SMDDS should be operated in *batch mode* since the solar energy can only be supplied intermittently and periodically. Furthermore, the freshwater demand of SMDDS is assumed to be time variant, thus the traditional continuous operation is almost out of the question in this study.

Obviously, a good SMDDS design should be not only cost optimal but also operable in a realistic environment. Although successful applications of the solar-driven

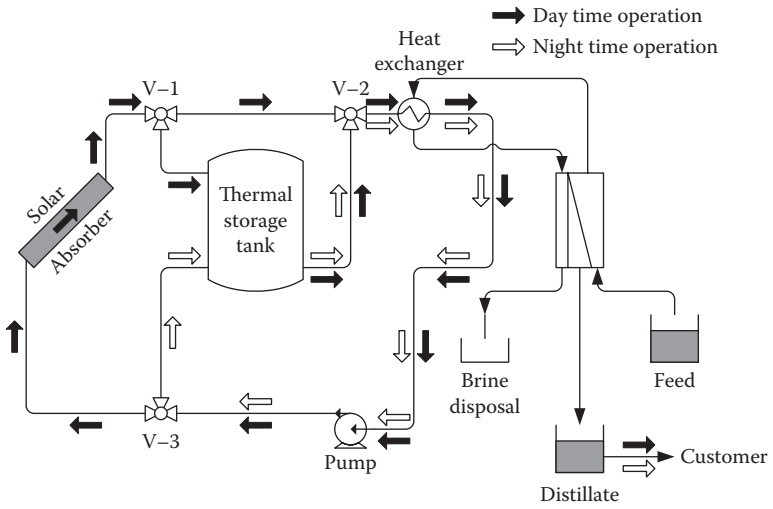

FIGURE 10.1 A typical SMDDS design—Configuration I.

AGMD modules were reported in the literature, these works focused primarily on thermal efficiency while the important issues concerning *operational flexibility* have not been addressed rigorously. Notice that the term "flexibility" is generally regarded as a system's capability of ensuring feasible operation over a specified region in the uncertain parameter space (Halemane and Grossmann, 1983). The sources of uncertainties may be either external or internal. Typical examples of the former case can be changes in throughput, feed quality, product demand, ambient conditions, and so forth, whereas the latter uncertainties are often associated with equipment deterioration, such as exchanger fouling and catalyst deactivation. Traditionally, the operational flexibility of a process is ensured in an ad hoc fashion by choosing conservative operating conditions, applying empirical overdesign factors, and introducing spare units. The major disadvantages of this approach can be summarized as follows:

i. Since the interactions among units are not considered, the actual flexibility level of the entire process cannot be accurately determined.
ii. Since the economic penalties of the heuristic design practices are not evaluated, their financial implications cannot be properly assessed.

A number of mathematical programming models have already been developed to facilitate quantitative flexibility analysis so as to provide the designers with the capabilities to (1) determine the performance index of any system design in relation to the expected operational requirements, (2) identify the bottleneck conditions which limit the flexibility in a design, and (3) compare alternative designs on an objective basis (Swaney and Grossmann, 1983a). Three performance measures for the steady-state, dynamic, and temporal flexibilities are discussed in this chapter. The first index is used primarily for gauging the continuous processes (Pistikopoulos and Grossmann, 1988a,b; 1989a,b; Petracci, et al., 1996), whereas the second is for the dynamic systems (Dimitriadis and Pistikopoulos, 1995). By considering the cumulative effects of uncertain disturbances over time, the programming model for computing the temporal flexibility index can be constructed by modifying its dynamic counterpart (Adi and Chang, 2013). Finally, note that the flexible SMDDS designs are identified in the present work on the basis of this last version of flexibility analysis. Q1

10.1 STEADY-STATE FLEXIBILITY ANALYSIS

Design and control decisions are usually made in two consecutive steps over the life cycle of a *continuous* chemical process. In the design phase, the "optimal" operating conditions and the corresponding material- and energy-balance data are determined traditionally on the basis of economic considerations. Since it is often desirable to address the operability issues at the earliest possible stage, the systematic incorporation of flexibility analysis in process synthesis and design has received considerable attention in recent years (Grossmann and Halemane, 1982; Halemane and Grossmann, 1983; Swaney and Grossmann, 1985a,b; Dimitriadis and Pistikopoulos, 1995; Bansal et al., 2000, 2002; Floudas et al., 2001). As mentioned before, these so-called uncertainties, referred to as its *operational flexibility,* may arise either from

random exogenous disturbances (such as those in feed qualities, product demands, environmental conditions, and so forth) from uncharacterized variations in the internal parameters (such as heat transfer coefficients, reaction rate constants, and other physical properties) (Malcom et al., 2007; Lima and Georgakis, 2008; Lima et al., 2010a,b), or the ability of a chemical process to maintain feasible operation despite uncertain deviations from the nominal state. The so-called *flexibility index* (FI_s) was first proposed by Swaney and Grossmann (1985a,b) to provide a quantitative measure of the feasible region in the parameter space. More specifically, FI_s can be associated with the maximum allowable deviations of the uncertain parameters from their nominal values, by which feasible operation can be assured with the proper manipulation of the control variables. The aforementioned authors also showed that, under certain convexity assumptions, critical points that limit feasibility and/or flexibility must lie on the vertices of the uncertain parameter space. Grossmann and Floudas (1987) later exploited the fact that sets of active constraints are responsible for limiting the flexibility of a design and developed a mixed integer nonlinear programming (MINLP) model accordingly. To this end, various approaches to facilitate flexibility analysis have been proposed in numerous studies published in the literature (Grossmann and Halemane, 1982; Halemane and Grossmann, 1983; Swaney and Grossmann, 1985a,b; Grossmann and Floudas, 1987; Varvarezos et al., 1995; Bansal et al., 2000, 2002; Floudas, et al., 2001; Ostrovski et al., 2001; Ostrovski and Volin, 2002; Volin and Ostrovski 2002; Malcom et al., 2007; Lima and Georgakis, 2008; Lima, et al., 2010a,b). Similar flexibility analysis was also carried out in a series of subsequent studies to produce resilient grassroots and revamp designs (Chang et al., 2009; Riyanto and Chang, 2010). Since the steady-state material-and-energy balances are used as the equality constraints in the aforementioned MINLP model (Swaney and Grossmann, 1985a,b; Grossmann and Floudas, 1987; Varvarezos et al., 1995; Ostrovski et al., 2001; Ostrovski and Volin, 2002; Volin and Ostrovski, 2002), this original index can be viewed as a performance indicator of the *continuous* process under consideration (Pistikopoulos and Grossmann, 1988a,b, 1989a,b; Petracci, et al., 1996), and it is referred to as the *steady-state flexibility index* in this chapter.

10.1.1 Model Formulation

As mentioned previously, the steady-state flexibility index was defined by Swaney and Grossmann (1985a,b) as an overall measure of the allowable variations in all uncertain parameters. The basic framework of the flexibility index model (Biegler et al., 1997) for computing such an index is outlined in the sequel.

For illustration clarity, let us first introduce two label sets:

$$\mathbb{I} = \{i \mid i \text{ is the label of an equality constraint}\} \tag{10.1}$$

$$\mathbb{J} = \{j \mid j \text{ is the label of an inequality constraint}\} \tag{10.2}$$

The general design model can be expressed accordingly as

$$h_i(\mathbf{d}, \mathbf{z}, \mathbf{x}, \theta) = 0 \quad \forall i \in \mathbb{I} \tag{10.3}$$

$$g_i(\mathbf{d},\mathbf{z},\mathbf{x},\theta) \le 0, \quad \forall j \in \mathbb{J} \tag{10.4}$$

where h_i is the i^{th} equality constraint in the design model (e.g., the mass or energy balance equation for a processing unit); g_j is the jth inequality constraint (e.g., a capacity limit); **d** represents a vector in which all design variables are stored; **z** denotes the vector of adjustable controlling variables; **x** is the vector of state variables; θ denotes the vector of uncertain parameters. **Q3**

The following mathematical program can be utilized to determine the so-called *feasibility function* ψ(**d**,θ), that is, **Q4**

$$\psi(\mathbf{d},\theta) = \min_{\mathbf{x},\mathbf{z}} \max_{j\in\mathbb{J}} g_j(\mathbf{d},\mathbf{z},\mathbf{x},\theta) \tag{10.5}$$

subject to the equality constraints given in Equation 10.3. Notice that this formulation means that, for a *fixed* design defined by **d** and the *fixed* parameters given in θ, the largest g_j ($\forall\, j \in \mathbb{J}$) is minimized by adjusting the control variables **z** while keeping $h_i = 0$ ($\forall i \in \mathbb{I}$). If ψ(**d**,θ) ≤ 0, then the given system is operable (see Figure 10.2).

On the other hand, the above optimization problem can be posed alternatively by introducing an extra scalar variable u, that is,

$$\psi(\mathbf{d},\theta) = \min_{\mathbf{x},\mathbf{z},u} u \tag{10.6}$$

subject to Equation 10.3 and

$$g_j(\mathbf{d},\mathbf{z},\mathbf{x},\theta) \le u \quad \forall\, j \in \mathbb{J} \tag{10.7}$$

Notice also that if ψ(**d**,θ) = 0, then at least one of the inequality constraints should be active, that is, $g_j = 0$ ($\exists\, j \in \mathbb{J}$).

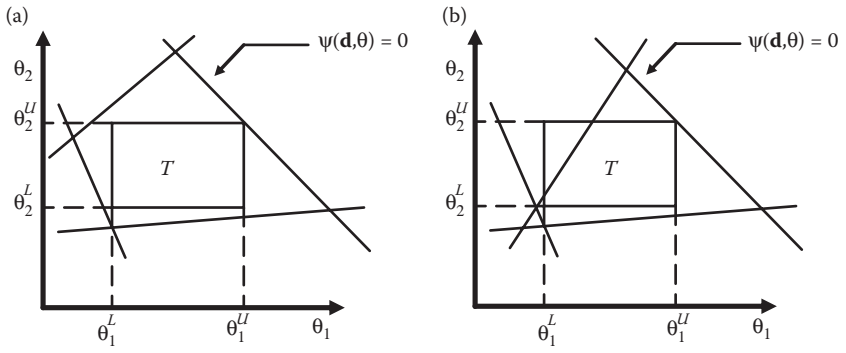

FIGURE 10.2 Feasible and infeasible designs in the parameter space. (Adapted from Biegler et al., 1987.) **Q19**

Since the aforementioned test can be performed only on deterministic models with constant θ, it is still necessary to develop an improved feasibility criterion by considering all possible values of the uncertain parameters. To this end, let us first define a feasible region **T** in the parameter space, that is,

$$\mathbf{T} = \left\{\theta | \theta^N - \Delta\theta^- \le \theta \le \theta^N + \Delta\theta^+\right\} \tag{10.8}$$

where θ^N denotes a vector of given nominal parameter values and $\Delta\theta^+$ and $\Delta\theta^-$ represent vectors of the expected deviations in the positive and negative directions, respectively. Hence, an additional optimization problem can be formulated to facilitate this modified test

$$\chi(\mathbf{d}) = \max_{\theta \in \mathbf{T}} \psi(\mathbf{d}, \theta) \tag{10.9}$$

where $\chi(\mathbf{d})$ denotes the feasibility function of a *fixed* design defined by **d** over the entire feasible region **T**. The given system should therefore be feasible if $\chi(\mathbf{d}) \le 0$, while infeasible if otherwise.

To develop a unified measure of the maximum tolerable range of variation in every uncertain parameter (Swaney and Grossmann, 1985a, b), the feasible region **T** is modified by introducing another scalar variable

$$\mathbf{T}(\delta) = \left\{\theta | \theta^N - \delta\Delta\theta^- \le \theta \le \theta^N + \delta\Delta\theta^+\right\} \tag{10.10}$$

where δ is a scalar variable to be determined by solving the flexibility index model given below

$$FI_s = \max \delta \tag{10.11}$$

subject to

$$\chi(\mathbf{d}) \le 0 \tag{10.12}$$

Note that the maximized objective value FI_s is the steady-state *flexibility index*, which represents the largest value of δ that guarantees $g_j \le 0$ ($\forall\, j \in \mathbb{J}$), that is, $\chi(\mathbf{d}) \le 0$, in the parameter space (see Figure 10.3).

10.1.2 Solution Strategies

Several effective strategies are available for solving the optimization problem defined by Equations 10.11 and 10.12. Two of them, that is, the active set method and the vertex method, are described in the sequel.

10.1.2.1 Active Set Method

Solving the flexibility index model is in general very difficult because Equations 10.11 and 10.12 represent a nonlinear, non-differentiable, multilevel optimization

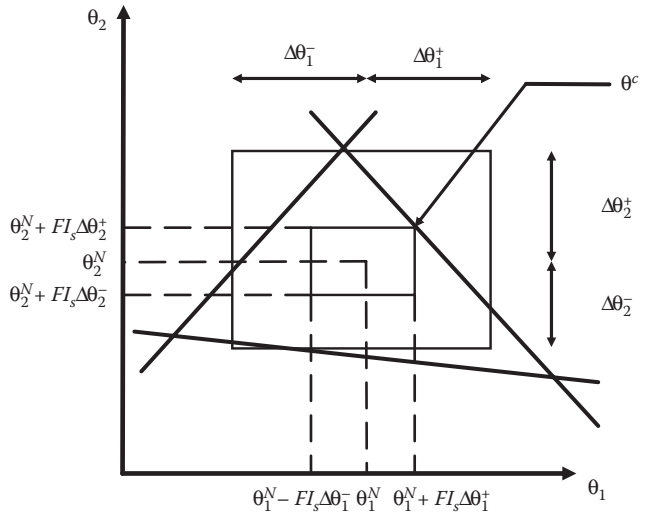

FIGURE 10.3 Geometrical interpretation of steady-state flexibility index. (Adapted from Biegler, L. T.; Grossmann I. E.; Westerberg, A. W. *Systematic Methods of Chemical Process Design*. Englewood Cliffs, New Jersey: *Prentice-Hall*, 690, **1997**.)

problem. Grossmann and Floudas (1987) developed a solution strategy on the basis of the Karush–Kuhn–Tucker (KKT) conditions of the optimization problem for computing the function $\psi(\mathbf{d},\theta)$, that is, Equations 10.3, 10.6, and 10.7. To be able to apply these conditions, the aforementioned flexibility index model is first reformulated by imposing an extra equality constraint that keeps the feasibility function zero, that is,

$$FI_s = \min \delta \tag{10.13}$$

subject to

$$\psi(\mathbf{d},\theta) = 0 \tag{10.14}$$

Notice that the original maximization problem, that is, Equations 10.11 and 10.12, is now replaced with the present *minimization* problem. This is owing to the fact that if the chosen value of δ is not the smallest, at least one inequality constraint must be violated, that is, $g_j > 0$ ($\exists\, j \in \mathbb{J}$). Since Equations 10.3 and 10.4 are inherently satisfied in the optimization problem defined by Equations 10.3, 10.6, and 10.7, the corresponding KKT conditions should be applicable. Consequently, the flexibility index problem in Equations 10.13 and 10.14 can be written more explicitly as follows (Grossman and Floudas, 1987):

$$FI_s = \min_{\delta,\mu_i,\lambda_j,s_j,y_j,x_i,z_k} \delta \tag{10.15}$$

subject to the constraints in Equation 10.3 and also those presented below

$$g_j(\mathbf{d},\mathbf{z},\mathbf{x},\theta) + s_j = 0, \quad j \in \mathbb{J} \tag{10.16}$$

$$\sum_{i\in\mathbb{I}} \mu_i \frac{\partial h_i}{\partial \mathbf{z}} + \sum_{j\in\mathbb{J}} \lambda_j \frac{\partial g_j}{\partial \mathbf{z}} = 0 \tag{10.17}$$

$$\sum_{i\in\mathbb{I}} \mu_i \frac{\partial h_i}{\partial \mathbf{x}} + \sum_{j\in\mathbb{J}} \lambda_j \frac{\partial g_j}{\partial \mathbf{x}} = 0 \tag{10.18}$$

$$\sum_{j\in\mathbb{J}} \lambda_j = 1 \tag{10.19}$$

$$\lambda_j - y_j \le 0, \quad j \in \mathbb{J} \tag{10.20}$$

$$s_j - Q(1 - y_j) \le 0, \quad j \in \mathbb{J} \tag{10.21}$$

$$\sum_{j\in\mathbb{J}} y_j = n_z + 1 \tag{10.22}$$

$$\theta^N - \delta\Delta\theta^- \le \theta \le \theta^N + \delta\Delta\theta^+ \tag{10.23}$$

$$y_j = \{0,1\}, \lambda_j \ge 0, s_j \ge 0, \quad j \in \mathbb{J} \tag{10.24}$$

$$\delta \ge 0 \tag{10.25}$$

where s_j is the slack variable for the jth inequality constraint; Q denotes a large enough positive number to be used as the upper bound of s_j;μ_i denotes the Lagrange multiplier of equality constraint h_i;λ_j is the Lagrange multiplier of inequality constraint g_j;y_j denotes the binary variable reflecting whether the corresponding inequality constraint is active, that is, $g_j = 0$ if $y_j = 1$, whereas $g_j < 0$ if $y_j < 0$; and n_z is the total number of independent controlling variables.

10.1.2.2 Vertex Method

The optimization procedure for Equations 10.11 and 10.12 can be greatly simplified if the optimal solution is always associated with one of the vertices of the feasible region $\mathbf{T}(\delta)$ (Halemane and Grossmann, 1983). Let $\Delta\theta^k$ ($\forall k \in V$) denote the kth vertex and V be the set of all vertices. Then the maximum value of δ along $\Delta\theta^k$ can be evaluated according to the following programming model:

$$\delta^k = \max_{\mathbf{x},\mathbf{z},\delta} \delta \tag{10.26}$$

subject to Equations 10.3, 10.4, and

$$\theta = \theta^N + \delta\Delta\theta^k \tag{10.27}$$

Among the corresponding parameter polyhedrons, that is, $\mathbf{T}(\delta^k), \forall k \in V$, it is clear that only the smallest one can be totally inscribed within the feasible region. Hence,

$$FI_s = \min_{k \in V} \left\{ \delta^k \right\} \tag{10.28}$$

Thus, the following simple procedure applies:

Step 1: Solve the optimization problem defined by Equations 10.3, 10.4, 10.26, and 10.27 for each vertex $k \in V$.
Step 2: Select FI_s according to Equation 10.28.

Swaney and Grossmann (1985a,b) showed that, only under certain convexity conditions for the constraints in Equations 10.3 and 10.4, the optimal solution is guaranteed to be associated with one of the vertices. However, even when these conditions are not met, it can often be found that this approach is still applicable. Note also that the vertex method may be quite impractical in realistic case studies due to dimension explosion. For example, $2^{10} = 1024$ optimization runs that are needed for 10 uncertain parameters and, if the number of parameters is raised to 20, the computation load for the required $2^{20} = 1{,}048{,}576$ runs can be overwhelming.

The implementation steps of steady-state flexibility analysis in water network designs can be found in Liou (2006). Owing to the special model structure for water network designs, Li and Chang (2011) suggested that a simplified version of the vertex method could be applied by checking only a single corner of the parameter space. This critical point should be associated with the upper or lower limit of each uncertain parameter on the basis of physical insights (Chang et al., 2009). Specifically, they are located at

- The upper bounds of the mass loads of water using units and the pollutant concentrations at the primary and secondary sources.
- The lower bounds of the removal ratios of wastewater treatment units, the allowed maximum inlet and outlet pollutant concentrations of water using units, and the allowed maximum inlet pollutant concentration of wastewater treatment units.

The flexibility index of a water network can thus be determined on the basis of this most constrained point alone.

10.2 DYNAMIC FLEXIBILITY ANALYSIS

As suggested by Dimitriadis and Pistikopoulos (1995), the operational flexibility of a *dynamic* system should be evaluated differently. By adopting a system of differential algebraic equations (DAEs) as the model constraints, these authors developed a

mathematical programming formulation for dynamic flexibility analysis. Clearly, this analysis is more rigorous than that based on the steady-state model since, even for a continuous process, the operational flexibility cannot be adequately characterized without accounting for the control dynamics. In an earlier study, Brengel and Seider (1992) advocated the need for design and control integration. The integration of flexibility and controllability in design was discussed extensively by several other groups (Chacon-Mondragon and Himmelblau, 1996; Mohideen et al., 1996; Bahri et al., 1997; Bansal et al., 1998; Georgiadis and Pistikopoulos, 1999; Aziz and Mujtaba, 2002; Malcolm et al., 2007). Soroush and Kravaris (1993a,b) addressed various issues concerning flexible operation for batch reactors. The effects of uncertain disturbances on the wastewater neutralization processes were also studied by Walsh and Perkins (1994). White et al. (1994) presented an evaluation method to assess the switchability of any given system, that is, its ability to perform satisfactorily when moving between different operating points. Dimitriadis et al. (1997) studied the feasibility problem from the safety verification point of view. Zhou et al. (2009) utilized a similar approach to assess the operational flexibility of batch systems.

10.2.1 Model Formulation

In the dynamic flexibility analysis, the equality constraints in Equation 10.3 are replaced with a system of differential-algebraic equations (Dimitriadis and Pistikopoulos, 1995), that is,

$$h_i\left(\mathbf{d}, \mathbf{z}(t), \mathbf{x}(t), \dot{\mathbf{x}}(t), \theta(t)\right) = 0 \quad \forall i \in \mathbb{I} \tag{10.29}$$

where $t \in [0, H], i \in \mathbb{I}$, and $\mathbf{x}(0) = \mathbf{x}^0$. On the other hand, the inequality constraints in Equation 10.4 should also be time dependent, that is,

$$g_j\left(\mathbf{d}, \mathbf{z}(t), \mathbf{x}(t), \theta(t)\right) \le 0 \quad \forall\, j \in \mathbb{J} \tag{10.30}$$

Finally, the uncertain parameters and their upper and lower limits in this case should be functions of time and Equation 10.10 can be modified as

$$\theta^N(t) - \delta\Delta\theta^-(t) \le \theta(t) \le \theta^N(t) + \delta\Delta\theta^+(t) \tag{10.31}$$

Thus, the corresponding *dynamic flexibility index* FI_d can be computed with the following model:

$$FI_d = \max \delta \tag{10.32}$$

subject to Equation 10.29 and

$$\max_{\theta(t)} \min_{\mathbf{z}(t)} \max_{j,t} g_j(\mathbf{d}, \mathbf{z}(t), \mathbf{x}(t), \theta(t)) \le 0 \tag{10.33}$$

Note that this model is essentially the dynamic version of Equations 10.11 and 10.12.

10.2.2 Solution Strategies

Two alternative strategies are presented in this section for computing the dynamic flexibility index. First of all, Equations 10.29, 10.32, and 10.33 can obviously be transformed into a steady-state flexibility index model by approximating the embedded differential equations with a set of algebraic equations. Another viable option is to establish the KKT conditions for the minimum feasibility functional and then develop the dynamic version of the active set method. These two approaches are outlined below.

10.2.2.1 Transformation to Steady-State FI Model through Discretization

The simplest strategy to compute the dynamic flexibility index is to convert the DAEs in Equation 10.29 into a system of algebraic equations on the basis of a credible numerical discretization technique. Since the resulting optimization problems should be identical to those described in Section 10.1.1, they can be solved with any existing algorithm for the steady-state flexibility analysis (see Section 10.1.2).

Two popular discretization techniques have been utilized in the past, that is, the differential quadrature (DQ) method (Bellman et al., 1971, 1972) and the orthogonal collocation (OC) method (Biegler, 1984; Cuthrell and Biegler, 1987). Since they were adopted for essentially the same purpose and both yield satisfactory results, let us consider only the former for the sake of brevity. Notice that the accuracy of DQ approximation has been well documented in the literature (e.g., Civan and Sliepcevich, 1984; Quan and Chang, 1989a,b; Chang et al., 1993), and its implementation procedure is also very straightforward. As pointed out by Shu (2000), DQ is essentially equivalent to the finite difference scheme of a higher order. To improve the computation efficiency when a large number of grid points are required, a localized DQ scheme was introduced by Zong and Lam (2002). An extensive discussion of differential quadrature and its state-of-the-art developments can be found in Zong and Zhang (2009).

To illustrate the DQ discretization principle, let us consider the first-order derivative of the ith state variable ($i \in \mathrm{I}$) as an example

$$\left.\frac{dx_i(t)}{dt}\right|_{t=t_m^e} \cong \sum_{n=1}^{N_{node}} w_{mn} x_i(t_n^e) \tag{10.34}$$

where $m = 1,2,\ldots,N_{node}$; $e = 1,2,\ldots,N_{element}$; t_m^e and t_n^e, respectively, denote the locations of the mth node and the nth node in time element e; w_{mn} denotes the weighting coefficient associated with the state value at t_n^e for the derivative at t_m^e, which is dependent only upon the *predetermined* node spacing. As a result, every differential equation in Equation 10.29 can be approximated with a set of algebraic equations. In addition, all inequality constraints in Equations 10.30 and 10.31 should be discretized at the node locations, that is,

$$g_j\left(\mathbf{d}, \mathbf{z}(t_m^e), \mathbf{x}(t_m^e), \theta(t_m^e)\right) \le 0 \quad \forall\, j \in \mathbb{J} \tag{10.35}$$

$$\theta^N(t_m^e) - \delta\Delta\theta^-(t_m^e) \le \theta(t_m^e) \le \theta^N(t_m^e) + \delta\Delta\theta^+(t_m^e) \tag{10.36}$$

Quan and Chang (1989a,b) suggested that, in most cases, it is beneficial to use the shifted zeros of a standard Chebyshev polynomial as the selected nodes. This node spacing in an arbitrary interval $t \in [a, b]$ yields the following formulas for calculating the weighting coefficients, that is,

$$w_{mn} = \frac{r_{N_{node}} - r_1}{b-a} \frac{(-1)^{(m-n)}}{r_m - r_n} \sqrt{\frac{1-r_n^2}{1-r_m^2}}, \quad m \ne n \tag{10.37}$$

$$w_{mm} = \frac{1}{2} \frac{r_{N_{node}} - r_1}{b-a} \frac{r_m}{(1-r_m^2)} \tag{10.38}$$

where $m,n = 1,2,\ldots,N_{node}$ and the locations of Chebyshev zeros in the standard interval [–1, +1] are

$$r_m = \cos\frac{(2m-1)\pi}{2N_{node}} \tag{10.39}$$

where w_{mn} are the weighting coefficients for the first-order derivatives. With these formulas, all weighting coefficients can be easily calculated for any combination of element length $b - a$ and node number N_{node}. A typical example can be found in Table 10.1.

As mentioned previously, the time horizon H is supposed to be divided into $N_{element}$ elements. Continuity of every state variable at the border point of each pair of adjacent elements can be enforced with a boundary condition, that is, $\mathbf{x}_k(t_{N_{node}}^e) = \mathbf{x}_k(t_1^{e+1})$ and $e = 1,2,\ldots,N_{element}$. The initial conditions of Equation 10.29 should be imposed at the left end of first element, that is, $\mathbf{x}_k(t_1^1) = \mathbf{x}_k^0$, whereas the states at right end of the last element are not constrained, that is, $\mathbf{x}_k(t_{N_{node}}^{N_{element}}) = \text{free}$. Finally, the element number and lengths should be allowed to be adjusted to achieve satisfactory accuracy.

10.2.2.2 Identification of Dynamic KKT Conditions

If one chooses *not* to discretize Equations 10.29 through 10.31 in the original formulation, then the corresponding feasibility functional can be defined in the same way as its steady-state counterpart in Equations 10.3, 10.6, and 10.7

TABLE 10.1
Weighting Coefficients for $b - a = 10$ and $N_{node} = 5$

n \ m	1	2	3	4	5
1	0.90085	–0.2	0.061803	–0.04721	0.1
2	1.37082	0.050203	–0.2618	0.161803	–0.32361
3	–0.647214	0.4	3.57E-34	–0.4	0.647214
4	0.32361	–0.1618	0.261803	0.050203	–1.37082
5	–0.1	0.047214	–0.0618	0.2	0.900854

$$\psi\left(\mathbf{d},\theta(t)\right) = \min_{\mathbf{x}(t),\mathbf{z}(t),u(t)} u(t)\Big|_{t=H} \tag{10.40}$$

subject to the constraints in Equation 10.29 and

$$\dot{u}(t) = 0 \tag{10.41}$$

$$g_j\left(\mathbf{d},\mathbf{z}(t),\mathbf{x}(t),\theta(t)\right) \le u(t) \quad \forall\, j \in \mathbb{J} \tag{10.42}$$

To facilitate derivation of the KKT conditions for this functional optimization problem, let us rewrite Equation 10.29 more explicitly as

$$\dot{\mathbf{x}}(t) = \mathbf{f}_1\left(\mathbf{d},\mathbf{z}(t),\mathbf{x}(t),\theta(t)\right) \tag{10.43}$$

$$\mathbf{f}_2\left(\mathbf{d},\mathbf{z}(t),\mathbf{x}(t),\theta(t)\right) = \mathbf{0} \tag{10.44}$$

An aggregated objective functional can be constructed by introducing Lagrange multipliers to incorporate all constraints, that is,

$$L = u(H) + \int_0^H \left\{\mu_u(t)\left[0 - \dot{u}\right] + \mu(t)^T\left[\mathbf{f}_1 - \dot{\mathbf{x}}\right] + \nu(t)^T\mathbf{f}_2 + \lambda(t)^T\left[\mathbf{g} - u\mathbf{1}\right]\right\}dt \tag{10.45}$$

where $\mathbf{g} = [g_1\ g_2\ g_3\ \ldots]^T$, $\mathbf{1} = [1\,1\,1\ldots]^T$, and the multipliers $\mu_u(t)$, $\mu(t)$ and $\nu(t)$ are real numbers while $\lambda(t) \ge \mathbf{0}$. By taking the first variation of L and setting it to zero, the following four sets of necessary conditions can be obtained:

i. $\mathbf{x}(0) = \mathbf{x}_0$; $\mu(H) = \mathbf{0}$; $\mu_u(0) = 0$; $\mu_u(H) = 1$

ii. $\dot{\mu} = -\mu^T\left(\dfrac{\partial \mathbf{f}_1}{\partial \mathbf{x}}\right) - \nu^T\left(\dfrac{\partial \mathbf{f}_2}{\partial \mathbf{x}}\right) - \lambda^T\left(\dfrac{\partial \mathbf{g}}{\partial \mathbf{x}}\right)$; $\dot{\mu}_u = {}^T\mathbf{1}$

iii. $\dot{\mathbf{x}} = \mathbf{f}_1$; $\mathbf{f}_2 = \mathbf{0}$; $\dot{u} = 0$; $\lambda^T\left(\mathbf{g} - u\mathbf{1}\right) = 0$; $\lambda \ge \mathbf{0}$

iv. $\mu^T\left(\dfrac{\partial \mathbf{f}_1}{\partial \mathbf{z}}\right) + \nu^T\left(\dfrac{\partial \mathbf{f}_2}{\partial \mathbf{z}}\right) + \lambda^T\left(\dfrac{\partial \mathbf{g}}{\partial \mathbf{z}}\right) = \mathbf{0}^T$

By following the same rationale in developing the active set method for computing FI_s, that is, Equations 10.13 and 10.14, it is necessary to set $u(t) = 0$ and change conditions in (iii) to

$$\text{(iii)}'\ \dot{\mathbf{x}} = \mathbf{f}_1; \quad \mathbf{f}_2 = \mathbf{0}; \quad u = 0; \quad \lambda^T\mathbf{g} = 0; \quad \lambda \ge \mathbf{0}$$

.

Therefore, the dynamic flexibility index FI_d can be determined by minimizing δ while subject to the constraints in (i), (ii), (iii)′, (iv), and Equation 10.31.

10.3 TEMPORAL FLEXIBILITY ANALYSIS

As indicated previously, the nominal values of uncertain parameters and their anticipated positive and negative deviations are assumed in the dynamic flexibility analysis to be available in advance at every instance over the entire time horizon of operation life. However, while an ill-designed system may become inoperable due to instantaneous variations in some process parameters at certain instances, the cumulative effects of temporary disturbances in finite time intervals can also result in serious consequences. Although the latter scenario is usually ignored in dynamic flexibility analysis, it is in fact a more probable event in practical applications. To address this important issue, a mathematical programming model has been developed by Adi and Chang (2013) for computing the corresponding performance measure, which was referred to as the *temporal flexibility index*.

10.3.1 Model Formulation and Solution Strategies

Let us assume that the variations in uncertain parameters are possible only within a finite time interval $[t_0, t_1] \subset [0, H]$. To characterize the cumulative effects, let us integrate Equation 10.31 over this finite interval, that is,

$$-\delta\int_{t_0}^{t_1}\Delta\theta(\tau)^- d\tau \le \int_{t_0}^{t_1}(\theta(\tau)-\theta(\tau)^N)d\tau \le \delta\int_{t_0}^{t_1}\Delta\theta(\tau)^+ d\tau \tag{10.46}$$

Since the expected maximum deviations in uncertain parameters should be regarded as given information, the expected *net* positive and negative cumulated deviations over interval $[t_0, t_1]$ can also be computed in advance. Let us introduce the following definitions to simplify notation:

$$\Delta\Theta^- = \int_{t_0}^{t_1}\Delta\theta(\tau)^- d\tau \tag{10.47}$$

$$\Delta\Theta^+ = \int_{t_0}^{t_1}\Delta\theta(\tau)^+ d\tau \tag{10.48}$$

and

$$\Theta(t) = \int_{t_0}^{t}\theta((\tau)-\theta_{,}(\tau)^N)d\tau \tag{10.49}$$

Additional constraints can be imposed upon the accumulated effects of the instantaneous variations in the uncertain parameters so as to ensure operational safety. Specifically, Equation 10.46 can be expressed explicitly as follows:

$$-\delta\Delta\Theta^{-} \leq \Theta(t) \leq \delta\Delta\Theta^{+} \tag{10.50}$$

Furthermore, since the time interval $[t_0, t_1]$ itself may be uncertain, Equation 10.49 can be rewritten as

$$\frac{d}{dt}\Theta(t) = \theta(t) - \theta^{N}(t) \tag{10.51}$$

where $\Theta(0) = 0$ and $t \in [0, H]$. Equations 10.29, 10.33, 10.50, and 10.51 can then be used as the constraints of a mathematical programming model to determine the temporal flexibility index FI_t by maximizing the scalar variable δ. Notice also that, since the only difference between the mathematical models for computing FI_d and FI_t lies in the inequality constraints that bound the uncertain parameters, the solution approaches described in Section 10.2.2 should be very similar to those adopted in the present case. The detailed descriptions of these strategies are thus omitted for the sake of brevity. The theoretical implications of temporal flexibility index can be summarized as follows:

If $FI_t < 1$, then the given batch process cannot withstand at least some of the temporary disturbances that satisfy Equations 10.50 and 10.51. If otherwise, then the operation should always be successful.

10.4 FLEXIBLE SMDDS DESIGNS

A realistic SMDDS design is expected to be fully functional in the presence of uncertain sunlight radiation and fluctuating freshwater demand. In this section, the *temporal flexibility index* (FI_t) is adopted as the evaluation criterion of SMDDS designs. All units embedded in the typical design (see Configuration I in Figure 10.1) must be properly sized to achieve a target FI_t. In addition, alternative thermal storage schemes should be evaluated accordingly. The stripped-down version of SMDDS design in Figure 10.4 (Configuration II) can certainly be analyzed and compared with Configuration I, while installation of an extra thermal storage tank (say, on an additional bypass from solar absorber to heat exchanger and/or vice versa) can also be considered.

10.4.1 Simplified Mathematical Models

The essential SMDDS units, that is, the solar absorber, the thermal storage tank, the counter-flow shell-and-tube heat exchanger, the AGMD modules, and the distillate tank, are interconnected in a typical system to form two separate processing routes for seawater desalination and solar energy conversion, respectively. For implementation convenience, the unit models given in Chang et al. (2010) have been simplified (Adi and Chang, 2013) and outlined below:

10.4.1.1 Solar Absorber

The solar energy is converted into heat using the SMDDS solar absorber. Two basic assumptions are adopted in formulating its mathematical model: (i) the fluid

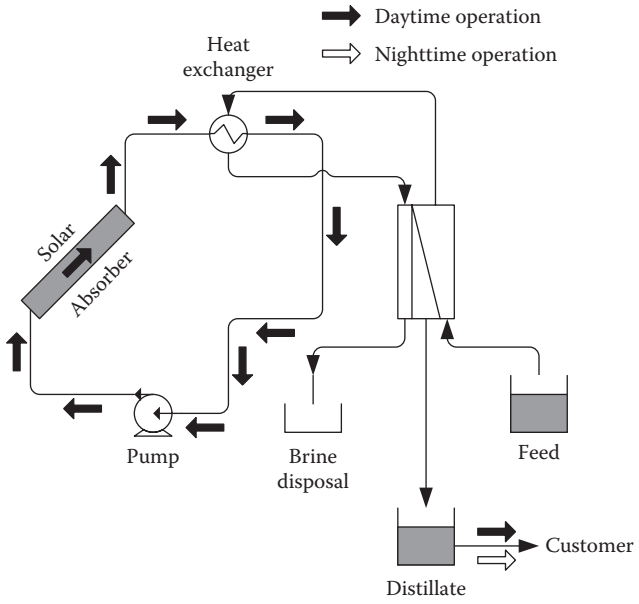

FIGURE 10.4 The stripped-down SMDDS design—Configuration II.

velocities in all absorber tubes are the same; (ii) the fluid temperature should be kept below 100°C; (iii) there is no water loss; and (iv) heat loss is negligible. The corresponding transient energy balance can be written as

$$\frac{dT_{f,SA_{out}}}{dt} = -L_{SA}\frac{\dot{m}_{f,SA}}{M_{f,SA}}\frac{T_{f,SA_{out}} - T_{f,SA_{in}}}{L_{SA}} + \frac{A_{SA}I(t)}{M_{f,SA}Cp_f^L} \tag{10.52}$$

$$T_{f,SA_{out}} \leq T_{f,SA_{out}}^{\max} \tag{10.53}$$

where $T_{f,SA_{in}}$ and $T_{f,SA_{out}}$ denote the inlet and outlet temperatures (°C) of the solar absorber, respectively; $T_{f,SA_{out}}^{\max}$ is the maximum allowable outlet temperature (100°C); $M_{f,SA}$ denotes the total mass of operating fluid in the solar absorber (kg); $\dot{m}_{f,SA}$ denotes the overall mass flow rate of operating fluid in solar absorber (kg/h); L_{SA} is the length of an absorber tube (m); A_{SA} is the exposed area of solar absorber (m^2); Cp_f^L is the heat capacity of operating fluid (J/kg°C); $I(t)$ is the solar irradiation rate per unit area (W/m^2).

10.4.1.2 Thermal Storage Tank

Based on the assumption that (i) the fluid within the thermal storage tank is well mixed, (ii) the inlet and outlet flow rates are identical, and (iii) the heat capacity of operating fluid is independent of temperature, the energy balance around thermal storage tank can be expressed as

$$M_{f,ST}\frac{dT_{f,ST_{out}}}{dt} = r_{f,ST}\dot{m}_{f,STL}\left(T_{f,ST_{in}} - T_{f,ST_{out}}\right) \tag{10.54}$$

$$r_{f,ST} = \frac{\dot{m}_{f,ST}}{\dot{m}_{f,STL}} \tag{10.55}$$

where $T_{f,ST_{in}}$ and $T_{f,ST_{out}}$ denote the inlet and outlet temperatures (°C), respectively; $M_{f,ST}$ represents the total mass of operating fluid in the thermal storage tank (kg); $\dot{m}_{f,STL}$ is the total mass flow rate driven by the pump in the thermal loop (kg/h); $\dot{m}_{f,ST}$ is the throughput of thermal storage tank (kg/h) which equals $r_{f,ST}\dot{m}_{f,STL}$.

In Configuration I, the thermal storage tank is employed during the daytime and nighttime according to the corresponding flow direction mode. In other words,

$$\dot{m}_{f,SA} = \begin{cases} m_{f,STL} & \text{if } I(t) > 0 \text{ (day time)} \\ 0 & \text{if } I(t) = 0 \text{ (night time)} \end{cases} \tag{10.56}$$

As a result, the flow ratio defined in Equation 10.55 can be treated as an adjustable control variable in daytime operation, that is, $0 \le r_{f,ST}(t) \le 1$, while $r_{f,ST}(=1)$ is kept unchanged during nighttime.

Finally, in the case of the thermal storage tank that is not utilized, that is, Configuration II, there is really no need to distinguish the operation modes and thus one can simply fix $\dot{m}_{f,SA} = \dot{m}_{f,STL}$, and $r_{f,ST} = 0$. **Q7**

10.4.1.3 Heat Exchanger

The hot fluid used in the counter-flow heat exchanger comes from the thermal storage tank and/or solar absorber, whereas the cold fluid is the seawater. The heat exchanger is assumed to be always in steady-state and there is no heat loss. Thus, the unit model of heat exchanger can be written as

$$\dot{m}_{f,MD}(T_{f,HX,CL_{out}} - T_{f,HX,CL_{in}}) = \dot{m}_{f,HX,HL}(T_{f,HX,HL_{in}} - T_{f,HX,HL_{out}}) \tag{10.57}$$

where $\dot{m}_{f,HX,HL}$ is the mass flow rate of hot fluid (kg/h); $T_{f,HX,HL_{in}}$ and $T_{f,HX,HL_{out}}$, respectively, denote the inlet and outlet temperatures of hot fluid (°C); $\dot{m}_{f,MD}$ is the mass flow rate of seawater in membrane distillation loop (kg/h); $T_{f,HX,CL_{in}}$ and $T_{f,HX,CL_{out}}$, respectively, denote the inlet and outlet temperatures of the cold fluid (°C). Note that the mass flow rate of hot fluid is essentially the same as that in the thermal loops in both Configurations I and II, that is,

$$\dot{m}_{f,HX,HL} = \dot{m}_{f,STL} \tag{10.58}$$

An energy balance around the valve V-2 yields

$$T_{f,HX,HL_{in}} = (1 - r_{f,ST})T_{f,SA_{out}} + r_{f,ST}T_{f,ST_{out}} \tag{10.59}$$

Again, this equation is also valid in the above two structures. Finally, let us consider the outlet temperature of hot fluid. According to the flow direction in Configuration I, the hot fluid leaving the heat exchanger is recycled back to the solar absorber in the daytime operation and to the thermal storage tank during nighttime, the following constraints should be imposed:

$$T_{f,HX,HL_{out}} = \begin{cases} T_{f,SA_{in}} & \text{if } I(t) > 0 \text{ (day time)} \\ T_{f,ST_{in}} & \text{if } I(t) = 0 \text{ (night time)} \end{cases} \tag{10.60}$$

On the other hand, since Configuration II is not equipped with a thermal storage tank, only the first constraint in Equation 10.60 can be used in the corresponding model.

10.4.1.4 AGMD Module

A simplified model is adopted in this study for characterizing the AGMD unit. It is assumed that the mass flux of distillate across the membrane is a function of the rate of energy input. Specifically, this flux in a standard module can be expressed as

$$N_{mem} \doteq \frac{m_{f,MD} Cp_f^L \left(T_{f,HX,CL_{out}} - T_{f,HX,CL_{in}}\right)}{\text{STEC} \cdot A_{MD} \cdot n_{AGMD}} \tag{10.61}$$

where N_{mem} denotes the distillate flux (kg/m^2.h); A_{MD} is the fixed membrane area of a standard AGMD module (i.e., 10 m^2); n_{AGMD} is the total number of standard modules; and STEC is the *specific thermal energy consumption* constant (kJ/kg), which can be considered as the ratio between energy supplied by the heat exchanger and mass of the distillate produced (Burgess and Lovegrove, 2005; Banat et al., 2007).

The mass flux through the AGMD membrane is driven primarily by the vapor pressure differential. However, to simplify calculations the corresponding flux is assumed here to be roughly proportional to the temperature difference. Since Equation 10.61 is used essentially as an empirical relation in this case, it should be only valid within a finite range of the seawater flow rate. Consequently, $\dot{m}_{f,MD}$ is treated in this work as an adjustable control variable, which is allowed to vary ±10% from its nominal value

$$0.9\dot{m}_{f,MD}^N \leq \dot{m}_{f,MD} \leq 1.1\dot{m}_{f,MD}^N \tag{10.62}$$

Finally, note that the seawater entering the AGMD module should not be allowed to exceed a specified upper bound so as to avoid damaging the membrane, that is,

$$T_{f,HX,CL_{out}} \leq T_{f,HX,CL_{out}}^{\max} \tag{10.63}$$

where $T_{f,HX,CL_{out}}^{\max}$ is the upper bound othe f cold stream temperature at the outlet of heat exchanger (90°C).

10.4.1.5 Distillate Tank

The distillate tank is acting as the buffer for the fluctuating water demand. The corresponding model can be written as

$$\rho_f^L A_{DT} \frac{dh_{DT}}{dt} = \dot{m}_{f,DT_{in}} - \dot{m}_{f,DT_{out}} \tag{10.64}$$

where ρ_f^L is the distillate density (kg/m^3); A_{DT} is the cross-sectional area of distillate tank (m^2); h_{DT} is the height of liquid in distillate tank (m); $\dot{m}_{f,DT_{in}}$ and $\dot{m}_{f,DT_{out}}$ denote the inlet and outlet flow rates, respectively, (kg/h). Note that the inlet flow is produced by the AGMD unit, that is,

$$\dot{m}_{f,DT_{in}} = n_{AGMD} N_{mem} A_{MD} \tag{10.65}$$

Finally, the liquid height in the distillate tank should be maintained within a specified range, that is,

$$h_{DT,low} \leq h_{DT} \leq h_{DT,high} \tag{10.66}$$

where $h_{DT,low}$ and $h_{DT,high}$, respectively, denote the given lower and upper bounds (m). Equations 10.52 through 10.66 are then incorporated into the temporal flexibility index model described in Section 10.3 and solved to determine the value of temporal flexibility index FI_t.

10.4.2 Case Studies

The important role of temporal flexibility index in SMDDS design is demonstrated in the case studies presented below. Note that the specifications of a standard AGMD module are assumed to be the same as those given in Banat et al. (2007). The effluent of cold seawater flows into the shell side of a heat exchanger and then into the hot flow channel of the AGMD unit. Only water vapor can be transferred through the membrane pore because of the hydrophobic nature of porous membrane. Water vapor then is condensed on the wall surface of the cold seawater flow channel and then collected in a distillate tank for domestic consumption.

The AGMD desalination unit is driven by the thermal energy which is circulated and carried in the operating fluid (which is water in the present case studies) as depicted in Figures 10.1 and 10.4. In the daytime operation, the heat generated by the solar absorber can be consumed entirely in either Configuration I or II if the irradiation level is low. In the case of strong sunlight, a portion of the absorbed energy can be kept in the thermal storage tank of Configuration I and then used later to enable an extended period of desalination operation after sunset. Since Configuration II is not equipped with any thermal storage facility, it is therefore necessary to utilize a relatively small absorber to ensure complete consumption of solar energy in daytime operation and satisfy the freshwater demand during the night with a large enough distillate tank.

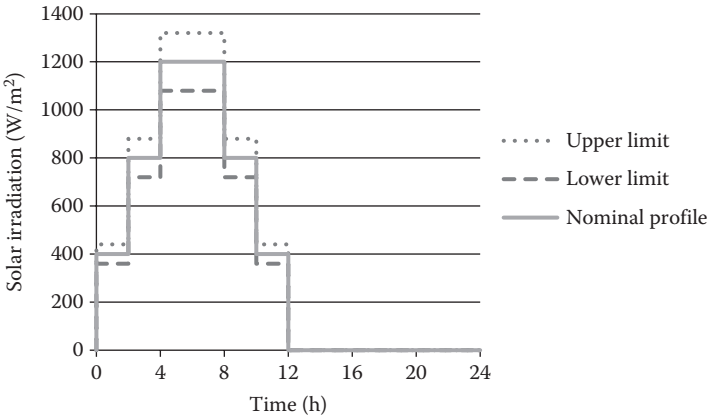

FIGURE 10.5 Solar irradiation profile.

There are two uncertain parameters considered in this case study. First is the solar irradiation rate $I(t)$ and the corresponding nominal profile $I^N(t)$, the expected upper and lower bounds are all depicted in Figure 10.5. Note that the expected positive and negative deviations at any time are both set at 10% of the nominal level. The other uncertainty parameter is the water demand rate $\dot{m}_{f,DT_{out}}(t)$ with the nominal value set at 18 kg/h × *wdf*(*t*). *wdf*(*t*) is the ratio between the demand rate at time *t* and a reference value, that is, 18 kg/h. The expected deviations in $m_{f,DT_{out}}$ are also selected to be 10% of its nominal value. The nominal level of *wdf*(*t*) and also the corresponding upper and lower limits are sketched in Figure 10.6 where the time-dependent household water consumption rate can be closely characterized according to the nominal profile of *wdf*(*t*). Better designs may be acquired accurately when more realistic solar irradiation and water demand profiles are available and they can be easily incorporated in the temporal flexibility analysis formulation.

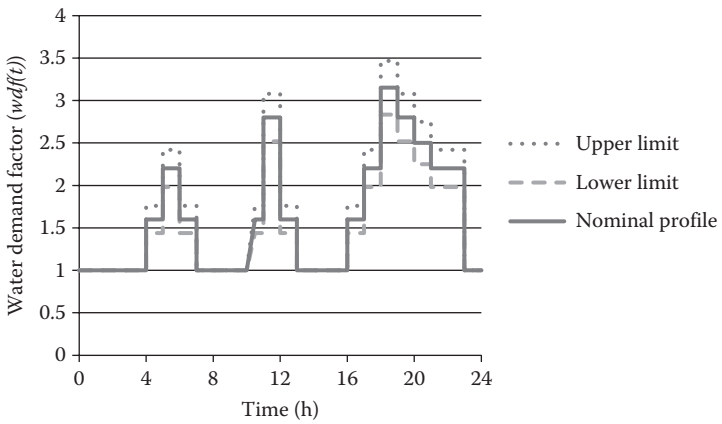

FIGURE 10.6 Normalized water demand profile.

On the basis of Equations 10.61 and 10.65, the production rate of each AGMD module at $T_{f,HX,CL_{out}} = 74°C$ is estimated to be 16.54 kg/h (Banat et al., 2007) (assuming that the feed temperature is $T_{f,HX,CL_{in}}$ 25°C). The nominal mass flow rate of seawater in membrane distillation loop $\dot{m}^N_{f,MD}$ is set to be 1125 kg/h per AGMD module according to Banat et al. (2007). Moreover, a maximum daily demand of 750.42 kg/day can be computed according to Figure 10.6. By adopting an average online period of 12 h/day, the approximate number of parallel AGMD modules can be calculated: $n_{AGMD} = (750.42/16.54 \times 12) = 3.78 \approx 4$, thus the total membrane area is 40 m^2. In the solar absorber, the total mass of operating fluid per unit area, that is, $M_{f,SA}/A_{SA}$, is set to be 15 kg/m^2 (Chang et al., 2010). The flow rate in the solar thermal loop ($\dot{m}_{f,STL}$) is set to be 36,000 kg/h, which is eight times the total nominal flow rate of seawater in the membrane distillation loop $\left(\dot{m}^N_{f,MD} = 1125 \times 4 = 4500\,\text{kg/h}\right)$ to ensure quick temperature response in the desalination loop. The volume of the distillate tank in each configuration is assumed to be ($A_{DT} = 0.35\,\text{m}^2$; $h_{DT,low} = 0\,\text{m}$; $h_{DT,high} = 2.143\,\text{m}$), whereas a 10 m^3 thermal storage tank ($M_{f,ST} = 10{,}000$ kg) is utilized in Configuration I. Finally, it is assumed that the heat capacity of operating fluid Cp^L_f is held constant at 4200 J/kg°C and its density ρ^L_f is also assumed to be constant at 1000 kg/m^3.

To facilitate a proper decision, the asymptotic energy utilization ratio between the solar absorber and the AGMD capacity is formulated as follows:

$$\begin{aligned}\phi_{util} &= \frac{\text{Maximum supply rate of solar energy}}{\text{Maximum consumption rate of thermal energy}} \\ &= \frac{A_{SA} I(t)^{\max}}{\dot{m}^{\max}_{f,MD} Cp^L_f (T^{\max}_{f,HX,CL_{out}} - T^{\min}_{f,HX,CL_{in}})}\end{aligned} \tag{10.67}$$

Hence, the energy collected by the solar absorber can be fully utilized by the AGMD module if $\phi_{util} \le 1$ and the excess heat need to be stored when $\phi_{util} > 1$. From Figure 10.5, it can be observed that $I(t)^{\max} = 1320$ W/m^2. On the basis of Equation 10.62, one could deduce $\dot{m}^{\max}_{f,MD} = 1.1\dot{m}^N_{f,MD} = 1237.5$ kg/h. Moreover, from the model description given in Section 10.4.1, it is reasonable to assume that $T^{\max}_{f,HX,CL_{out}} = 90°C$ and $T^{\min}_{f,HX,CL_{in}} = 25°C$. For a given ϕ_{util}, the calculation for the solar absorber size is simply straightforward according to Equation 10.67. For example, the absorber area for $\phi_{util} = 1$ should be $A_{SA} = (1237.5 \times 4200 \times (90 - 25)/1320 \times 3600) = 71.09\,\text{m}^2$. For the sake of completeness, all model parameters and variables used in the case studies are also listed in Table 10.2.

Given an AGMD module size, the solar absorber can be sized on the basis of Equation 10.67. By adopting the aforementioned thermal storage tank and distillate tank, the temporal flexibility indices of Configurations I and II can be computed for different utilization ratios. Table 10.3 summarizes the corresponding optimization results. It can be seen that when $\phi_{util} \le 1$ the same flexibility indices can be obtained with both configurations. This is because the absorbed solar energy is consumed almost immediately and completely, therefore, the thermal storage tank in Configuration I is not needed at all, that is, $r_{f,ST} = 0$. On the other hand, one can see that $r_{f,ST} = 1$ if $\phi_{util} > 1$, which implies that the thermal storage tank is fully utilized for storing the excess solar energy acquired during daytime operation in Configuration I. Q8

TABLE 10.2
Model Parameters and Variables

Symbol	Definition	Value	Classification
$T^{\max}_{f,SA_{out}}$	Maximum allowable outlet temperature of solar absorber	100°C	**d**
$M_{f,SA}$	Total mass of operating fluid in solar absorber	–	**d**
L_{SA}	Length of absorber tube	–	**d**
A_{SA}	Exposed area in solar absorber	–	**d**
Cp^{L}_{f}	Heat capacity of operating fluid	4200 J/kg°C	**d**
$M_{f,ST}$	Total mass of operating fluid in thermal storage tank	10,000 kg	**d**
$\dot{m}_{f,STL}$	Mass flow rate in thermal loop	36,000 kg/h	**d**
$T_{f,HX,CL_{in}}$	Cold fluid inlet temperature of heat exchanger	25°C	**d**
A_{MD}	Membrane area of standard AGMD module	10 m^2 [36]	**d**
n_{AGMD}	Total number of standard AGMD modules	–	**d**
STEC	Specific Thermal Energy Consumption	14,000 kJ/kg [36]	**d**
$T^{\max}_{f,HX,CL_{out}}$	Maximum cold fluid outlet temperature of heat exchanger	90°C	**d**
ρ^{L}_{f}	Distillate density	1000 kg/m^3	**d**
A_{DT}	Cross-sectional area of distillate tank	0.35 m^2	**d**
$h_{DT,low}$	Lower bound of liquid height in distillate tank	0 m	**d**
$h_{DT,high}$	Upper bound of liquid height in distillate tank	2.14 m	**d**
ϕ_{util}	Energy utilization ratio	To be selected	**d**
$I(t)^{\max}$	Maximum solar irradiation rate per unit area	1320 W/m^2	**d**
$\dot{m}^{\max}_{f,MD}$	Maximum mass flow rate in membrane distillation loop	1237.5 kg/h	**d**
$T^{\min}_{f,HX,CL_{in}}$	Minimum cold fluid inlet temperature of heat exchanger	25°C	**d**
$T_{f,SA_{in}}$	Inlet temperature of solar absorber	–	**x**
$T_{f,SA_{out}}$	Outlet temperature of solar absorber	–	**x**
$m_{f,SA}$	Mass flow rate of operating fluid in solar absorber	–	**x**
$T_{f,ST_{in}}$	Inlet temperature of thermal storage tank	–	**x**
$T_{f,ST_{out}}$	Outlet temperature of thermal storage tank	–	**x**
$\dot{m}_{f,ST}$	Throughput of thermal storage tank	–	**x**
$r_{f,ST}$	Flow ratio for thermal storage tank	–	**x**
$\dot{m}_{f,HX,HL}$	Mass flow rate of hot fluid in heat exchanger	–	**x**
$T_{f,HX,HL_{in}}$	Hot fluid inlet temperature of heat exchanger	–	**x**
$T_{f,HX,HL_{out}}$	Hot fluid outlet temperature of heat exchanger	–	**x**
$T_{f,HX,CL_{out}}$	Cold fluid outlet temperature of heat exchanger	–	**x**
h_{DT}	Liquid height in distillate tank	–	**x**
$\dot{m}_{f,DT_{in}}$	Inlet flow rate of distillate tank	–	**x**
N_{mem}	Distillate flux through AGMD membrane	–	**x**
$\dot{m}_{f,MD}$	Mass flow rate in membrane distillation loop	4500 kg/h (nominal)	**z**
I	Solar irradiation rate per unit area	–	θ
$\dot{m}_{f,DT_{out}}$	Outlet flow rate of distillate tank	–	θ

TABLE 10.3
Optimization Results

	Case No.	1	2	3	4	5	6	7
Configuration	ϕ_{util}	0.785	0.955	1	1.16	1.28	1.385	1.576
	FI_t	0	1	1.24	1.65	1.65	1	0
I	$r_{f,ST}$ (day)	0	0	0	1	1	1	1
	$g_j = 0$	$h_{DT,low}$	$h_{DT,low}$	$h_{DT,low}$	$h_{DT,low}$	$h_{DT,high}$	$h_{DT,high}$	$h_{DT,high}$
	$\dot{m}_{f,MD}$ factor	1.1	1.1	1.1	1.1	0.9	0.9	0.9
	FI_t	0	1	1.24	1	0	inf	Inf
II	$r_{f,ST}$ (day)	0	0	0	0	0	N/A	N/A
	$g_j = 0$	$h_{DT,low}$	$h_{DT,low}$	$h_{DT,low}$	$T^{\max}_{f,SA_{out}}$	$T^{\max}_{f,SA_{out}}$	N/A	N/A
	$\dot{m}_{f,MD}$ factor	1.1	1.1	1.1	1.1	1.1	N/A	N/A

Note that, although $r_{f,ST}$ is allowed to assume a real value between 0 and 1 in this situation, this optimal operating policy is adopted mainly to avoid violating the temperature upper bounds in Equations 10.53 and 10.63.

Notice that the information of the active constraint in each optimum solution can also be found in Table 10.3. When $\phi_{util} < 1$, the consumed energy may not be enough to meet the demand; hence, the distillate tank is expected to be empty sometimes. The optimization results of the corresponding two cases are analyzed below: **Q9**

1. Let us first consider Case 1 when $\phi_{util} = 0.785$. Note that $FI_t = 0$ in this case, that is, no deviations from the nominal parameters are allowed for both configurations. This is due to the fact that the nominal absorption rate of solar energy is just enough to meet the nominal demand by maximizing the control variable $\dot{m}_{f,MD}$ at all times.
2. Let us next consider Case 2 when $\phi_{util} = 0.955$. Note that $FI_t = 1$ in this case, that is, the expected deviations from the nominal parameters can be exactly accommodated in both configurations. To validate this prediction, the worst-case scenario (which is corresponding to the lower bound of solar irradiation rate and the upper bound of water demand rate) has been numerically simulated with Simulink® (The Mathworks, Inc., 2012). The Simulink program was built according to Equations 10.52 through 10.66 and also the parameter values listed in Table 10.2. To facilitate the simulation run, three time profiles were adopted as inputs, that is, (1) the lower limit of the solar irradiation profile in Figure 10.5, (2) the upper limit of the water demand profile in Figure 10.6, and (3) the control variable $\dot{m}_{f,MD}(t)$ obtained by solving the temporal flexibility index model. The simulated temperature of operating fluid at the exit of the solar absorber (i.e., $T_{f,SA_{out}}$) and also that of seawater at the exit of the heat exchanger (i.e., $T_{f,HX,CL_{out}}$) are both plotted in Figure 10.7. It can be clearly observed that, both temperatures are always well below their respective upper bounds. The corresponding water level in the distillate tank can also be found in Figure 10.8. Note that the tank is

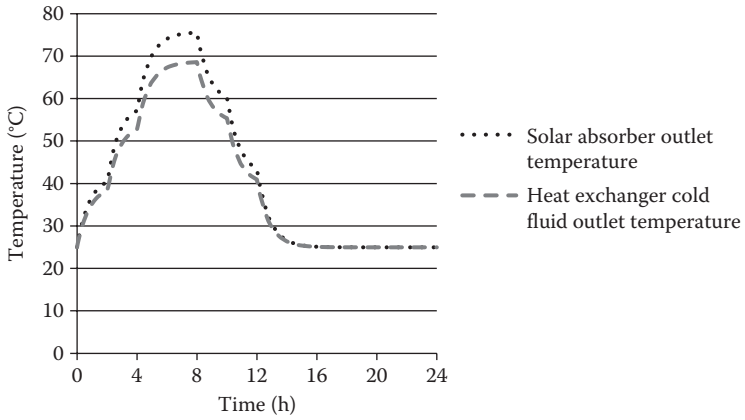

FIGURE 7 The time profiles of $T_{f,SA_{out}}$ and $T_{f,HX,CL_{out}}$ for both configurations in the worst-case scenario ($\phi_{util} = 0.955$).

just emptied at the end of 24 h. This observation essentially confirms the optimization result of $FI_t = 1$ for both configurations. Thus, if the desired value of temporal flexibility index is one, Configuration II should be chosen since the equipment cost of thermal storage facility can be saved.

3. In Case 3 when $\phi_{util} = 1$, notice that the optimization results are still the same for both configurations, that is, $r_{f,ST} = 0$ in daytime operations and $FI_t = 1.24$. If the target value of temporal flexibility index is 1, then Configurations I and II in this case are both slightly overdesigned since $FI_t > 1$. However, if a higher operational flexibility is called for in the design, then there is an incentive to consider additional cases where the solar absorbers are larger, that is, $\phi_{util} > 1$. Following are the corresponding case studies:

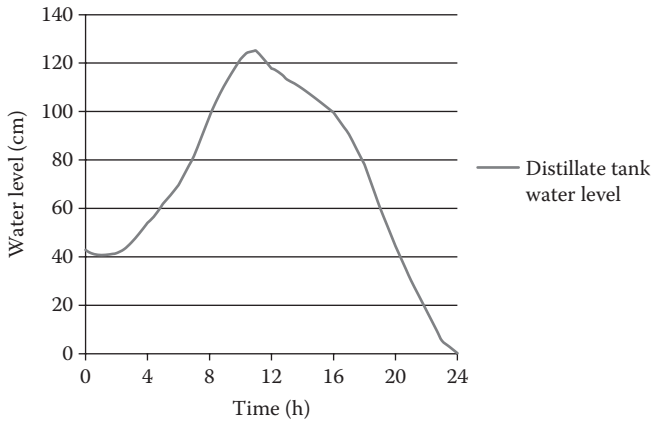

FIGURE 10.8 The time profiles of h_{DT} for both configurations in the worst-case scenario ($\phi_{util} = 0.955$).

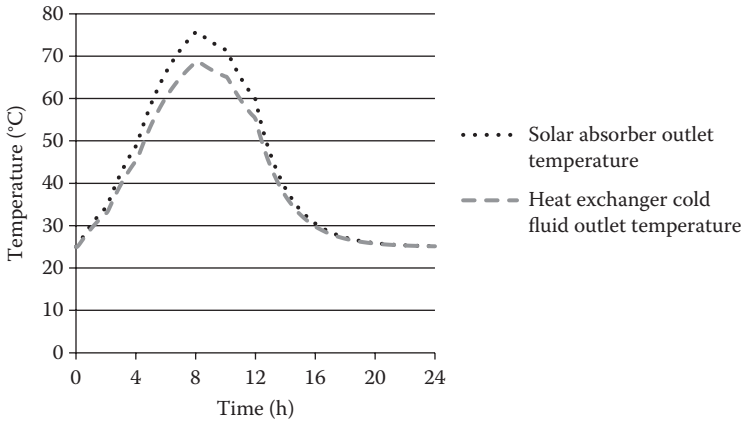

FIGURE 10.9 The time profiles of $T_{f,SA_{out}}$ and $T_{f,HX,CL_{out}}$ for Configuration I in the worst-case scenario ($\phi_{util} = 1.16$).

4. In Case 4 ($\phi_{util} = 1.16$), Configuration I can be made more flexible ($FI_t = 1.65$) by operating the thermal storage tank, that is, $r_{f,ST} = 1$. The corresponding worst-case scenario can be simulated and the time profiles of three critical variables, that is, $T_{f,SA_{out}}$, $T_{f,HX,CL_{out}}$, and h_{DT}, can be found in Figures 10.9 and 10.10. On the other hand, note that the temporal flexibility index of Configuration II equals one. This is because, since there is no thermal storage capacity, the exit temperature of the solar absorber ($T_{f,SA_{out}}$) reaches its upper limit at a certain instance during daytime operation. The corresponding system behavior can be characterized with Figures 10.11 and 10.12.
5. In Case 5 ($\phi_{util} = 1.28$), the temporal flexibility index of Configuration I can be raised to 1.65 and the active constraint is now associated with the upper

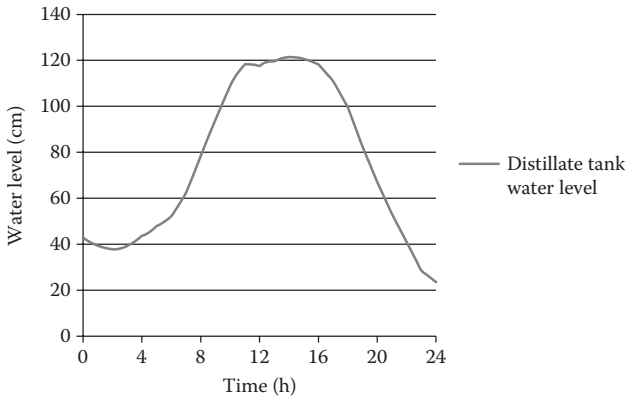

FIGURE 10.10 The time profile of h_{DT} for Configuration I in the worst-case scenario ($\phi_{util} = 1.16$).

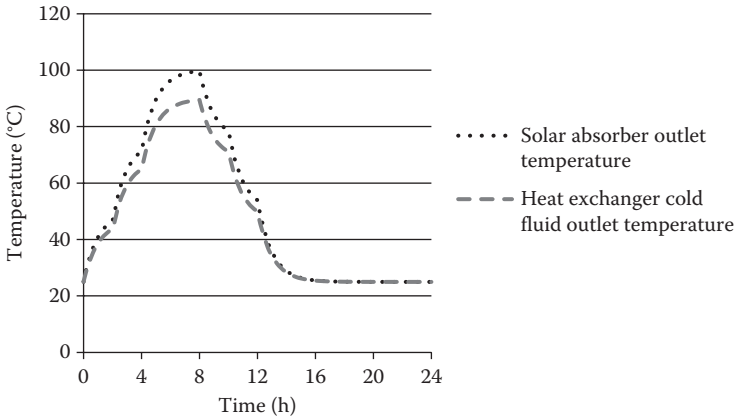

FIGURE 10.11 The time profiles of $T_{f,SA_{out}}$ and $T_{f,HX,CL_{out}}$ for Configuration II in the worst-case scenario ($\phi_{util} = 1.16$).

bound of water level in the distillate tank, that is, $h_{DT} \leq h_{DT,high}$. This is obviously due to the fact that the solar energy is introduced at a rate that is much faster than the consumption rate of thermal energy. On the other hand, note that $FI_t = 0$ for Configuration II. This drastic reduction of flexibility can also be attributed to the high intake rate of solar energy. Since there is no thermal storage tank, it is very difficult to keep the exit temperature of the solar absorber ($T_{f,SA_{out}}$) below 100°C.

6. In Case 6 ($\phi_{util} = 1.385$) and Case 7 ($\phi_{util} = 1.576$), the selected solar absorbers are larger than those used in the other cases. Since more water is produced in Configuration I while the size of distillate tank remains the same in either Case 6 or 7, the resulting flexibility index becomes much

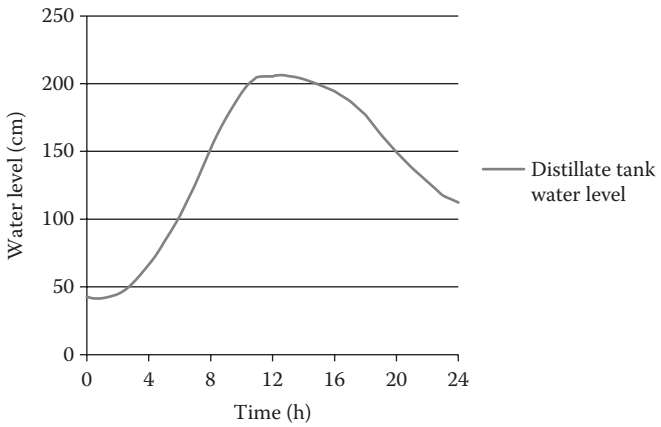

FIGURE 10.12 The time profile of h_{DT} for Configuration II in the worst-case scenario ($\phi_{util} = 1.16$).

lower than that achieved in Case 5. On the other hand, note that $FI_t = 0$ for Configuration II in Case 5. Thus, any further increase in the utilization ratio inevitably renders Configuration II infeasible.

If there is a need to make the SMDDS system even more flexible ($FI_t > 1.65$), one can deduce from Case 5 that this goal can be reached by relaxing the active constraint, that is, by enlarging the thermal storage tank ($M_{f,ST} \geq 10{,}000$ kg) and also the distillate tank ($h_{DT,high} \geq 2.143$ m). Finally, it should be noted that the temporal flexibility may be further enhanced by introducing additional structural modifications, for example, by operating more than one thermal storage tank in parallel. The merits of these new configurations can be easily assessed on the basis of the proposed temporal flexibility analysis.

10.5 CONCLUDING REMARKS AND UNSETTLED ISSUES

Three different types of flexibility analyses are discussed in this chapter with emphases on their model formulations and solution strategies. Specifically,

1. For the steady-state flexibility analysis, the available basic formulation (Swaney and Grossmann, 1985a, b) is presented for quantifying the ability of any continuous process to maintain feasible operation under uncertainty influences. Two main strategies are described for solving the corresponding multilevel optimization problems. On the basis of KKT conditions for the lower levels, a single-level formulation can be derived to compute the steady-state flexibility index FI_s. Another approach to achieve the same purpose is the so-called vertex method, which is valid if the solution lies on one of the vertices of the feasible region $\mathbf{T}(\delta)$ in the parameter space (Halemane and Grossmann, 1983). This method can also be further simplified when physical insights (Chang et al., 2009) are available for eliminating the unlikely candidates (Li and Chang, 2011).
2. The conventional formulation for the dynamic flexibility analysis (Dimitriadis and Pistikopoulos, 1995) is also described briefly in this chapter. Since the system dynamics are characterized with DAEs in the model constraints, the required solution strategies must be devised accordingly. In the first approach, a discretization method, for example, the DQ (Bellman et al., 1971, 1972), is adopted to convert the DAEs into a system of algebraic equations and solve the resulting model with existing strategies for the steady-state flexibility analysis. On the other hand, the KKT conditions can also be derived via calculus of variation to produce the dynamic version of the active set method.
3. For the temporal flexibility analysis, a novel concept of *temporal flexibility* has been developed to address the practical issues caused by short-term disturbances that may occur in operating the batch chemical plants. A generic mathematical programming model is formulated accordingly for characterizing the corresponding performance measure. The solution strategies in this case are essentially the same as those for the dynamic flexibility analysis.

The usefulness of the above analyses is demonstrated with a realistic application, that is, the SMDDS design problem where several design alternatives are evaluated according to their temporal flexibility indices. Although satisfactory results are obtained in this work, there are still several unsettled issues which require further attention. Specifically,

1. In the case of the steady-state flexibility analysis, the uncertain parameter space is characterized according to Equation 10.8, that is, it is a hypercube bound by the following inequality constraints:

$$\theta^N - \Delta\theta^- \le \theta \le \theta^N + \Delta\theta^+$$

However, this space may be generalized to any region bound by

$$\psi(\theta) \le \mathbf{0}$$

where $\psi(\theta)$ is a vector of linear or nonlinear functions of θ.
2. Lai and Hui (2008) have developed a promising flexibility metric which was referred to as the volumetric flexibility (FI_v). It is defined according to the hypervolume ratio of the feasible region and the region containing all possible combinations of expected uncertain parameters. In certain applications, this index is believed to be capable of providing more reliable assessments of the system performance with relatively mild computation requirements. Since it was developed only for the steady-state processes, there seems to be a need for extending this approach for the dynamic problems.
3. The discretization strategy for solving dynamic flexibility index problems needs further improvement so as to enhance computational efficiency. The conventional DQ method (Bellman et al., 1971, 1972; Quan and Chang, 1989a, b) has been adopted with arbitrarily chosen grid points and elements. The computation loads were quite heavy, which is considered necessary to develop a systematic strategy to determine the minimum numbers of grid points and elements, the proper grid spacing, and the optimal element length(s) for solving the dynamic and temporal flexibility index models.

REFERENCES

Adi, V. S. K.; Chang, C. T. A mathematical programming formulation for temporal flexibility analysis. *Comput. Chem. Eng.*, *57*, 151, **2013**.

Adi, V. S. K.; Chang, C. T. SMDDS design based on temporal flexibility analysis. *Desalination*, *320*, 96, **2013**.

Aziz, N.; Mujtaba, I. M. Optimal operation policies in batch reactors. *Chem. Eng. J.*, *85*, 313, **2002**.

Bahri, P. A.; Bandoni, J. A.; Romagnoli, J. A. Integrated flexibility and controllability analysis in design of chemical processes. *AIChE J.*, *43*, 997, **1997**.

Banat, F.; Jwaied, N.; Rommel, M.; Koschikowski, J.; Wieghaus, M. Performance evaluation of the "Large SMADES" autonomous desalination solar-driven membrane distillation plant in Aqaba, Jordan. *Desalination*, *217*, 17, **2007**.

Bansal, V.; Perkins, J. D.; Pistikopoulos, E. N. Flexibility analysis and design of dynamic processes with stochastic parameters. *Comput. Chem. Eng.*, 22, S817, **1998**.

Bansal, V.; Perkins, J. D.; Pistikopoulos, E. N. Flexibility analysis and design of linear systems by parametric programming. *AIChE J.*, *46*, 335, **2000**.

Bansal, V.; Perkins, J. D.; Pistikopoulos, E. N. Flexibility analysis and design using a parametric programming framework. *AIChE J.*, *48*, 2851, **2002**.

Bellman, R. E.; Casti, J. Differential quadrature and long-term integration. *J. Math. Anal. Appl*., *34*, 235, **1971**.

Bellman, R. E.; Kashef, B. G.; Casti, J. Differential quadrature: A technique for the rapid solution of nonlinear partial differential equations. *J. Comput. Phys.*, *10*, 40, **1972**.

Ben Bacha, H.; Dammak, T.; Ben Abdalah, A. A.; Maalej, A. Y.; Ben Dhia, H. Desalination unit coupled with solar collectors and storage tank: Modeling and simulation. *Desalination*, *206*, 341, **2007**.

Biegler, L. T. Solution of dynamic optimization problems by successive quadratic programming and orthogonal collocation. *Comput. Chem. Eng*., *8*, 243, **1984**.

Biegler, L. T.; Grossmann I. E.; Westerberg, A. W. *Systematic Methods of Chemical Process Design*. Englewood Cliffs, New Jersey: Prentice-Hall, 690, **1997**.

Brengel, D. D.; Seider, W. D. Coordinated design and control optimization of nonlinear processes. *Comput. Chem. Eng.*, *16*, 861, **1992**.

Bui, V. A.; Vu, L. T. T.; Nguyen, M. H. Simulation and optimization of direct contact membrane distillation for energy efficiency. *Desalination*, *259*, 29, **2010**.

Burgess, G.; Lovegrove, K. Solar thermal powered desalination: Membrane versus distillation technologies. 2005. http://solar-thermal.anu.edu.au/files/2010/02/DesalANZSES05.pdf (Accessed April 2013). **Q10**

Cabassud C.; Wirth, D. Membrane distillation for water desalination: How to choose an appropriate membrane? *Desalination*, *157*, 307, **2003**.

Chacon-Mondragon, O. L.; Himmelblau, D. M. Integration of flexibility and control in process design. *Comput. Chem. Eng.*, *20*, 447, **1996**. **Q11**

Chang, C. T.; Li, B. H.; Liou, C. W. Development of a generalized mixed integer nonlinear programming model for assessing and improving the operational flexibility of water network designs. *Ind. Eng. Chem. Res.*, *48*, 3496, **2009**.

Chang, C. T.; Tsai, C. S.; Lin, T. T. Modified differential quadratures and their applications. *Chem. Eng. Commun.*, *123*, 135, **1993**.

Chang, H.; Lyu, S. G.; Tsai, C. M.; Chen, Y. H.; Cheng, T. W.; Chou, Y. H. Experimental and simulation study of a solar thermal driven membrane distillation desalination process. *Desalination*, *286*, 400, **2012**.

Chang, H.; Wang, G. B.; Chen, Y. H.; Li, C. C.; Chang, C. L. Modeling and optimization of a solar driven membrane distillation desalination System. *Renew. Energ*., *35*, 2714, **2010**.

Civan F.; Sliepcevich, C. M. Differential quadrature for multidimensional problems. *J. Math. Anal.Appl.*, *101*, 423, **1984**.

Cuthrell, J. E.; Biegler, L. T. On the optimization of differential algebraic process systems. *AIChE J*., 33, 1257, **1987**.

Dimitriadis, V. D.; Pistikopoulos, E. N. Flexibility analysis of dynamic systems. *Ind. Eng. Chem. Res.*, *34*, 4451, **1995**.

Dimitriadis, V. D.; Shah, N.; Pantelides, C. C. Modeling and safety verification of discrete/continuous processing systems. *AIChE J.*, *43*, 1041, **1997**.

Floudas, C. A.; Gunus, Z. H.; Ierapetritou, M. G. Global optimization in design under uncertainty: Feasibility test and flexibility ondex problems. *Ind. Eng. Chem. Res.*, *40*, 4267, **2001**.

Gálvez, J. B.; García-Rodríguez, L.; Martín-Mateos, I. Seawater desalination by an innovative solar-powered membrane distillation system: The MEDESOL project. *Desalination*, *246*, 567, **2009**.

Georgiadis, M. C.; Pistikopoulos, E. N. An integrated framework for robust and flexible process systems. *Ind. Eng. Chem. Res.*, *38*, 133, **1999**.

Grossmann, I. E.; Floudas, C. A. Active constraint strategy for flexibility analysis in chemical process. *Comput. Chem. Eng.*, *11*, 675, **1987**.

Grossmann, I. E.; Halemane, K. P. Decomposition strategy for designing flexible chemical plants. *AIChE J.*, *28*, 686, **1982**.

Guillen-Burrieza, E.; Blanco, J.; Zaragoza, G.; Alarcon, D. C.; Palenzuela, P.; Ibarra, M.; Gernjak, W. Experimental analysis of an air gap membrane distillation solar desalination pilot system. *J. Membr. Sci.*, *379*, 386, **2011**.

Halemane, K. P.; Grossmann, I. E. Optimal process design under uncertainty. *AIChE J.*, *29*, 425, **1983**.

Koschikowski, J.; Wieghaus, M.; Rommel, M. Solar thermal-driven desalination plants based on membrane distillation. *Desalination*, *156*, 295, **2003**.

Lai, S. M.; Hui, C. -W. Process flexibility for multivariable systems. *Ind. Eng. Chem. Res.*, *47*, 4170, **2008**.

Li, B. H.; Chang, C. T., 2011, Efficient flexibility assessment procedure for water network designs. *Ind. Eng. Chem. Res.*, 50, 3763, **2011**.

Lima F. V.; Georgakis C. Design of output constraints for model-based non-square controllers using interval operability. *J. Process Control*, 18, 610, **2008**.

Lima, F. V.; Georgakis C.; Smith, J. F.; Schnelle, P. D.; Vinson D. R. Operability-based determination of feasible control constraints for several high-dimensional nonsquare industrial processes. *AIChE J*., *56*, 1249, **2010a**.

Lima, F. V.; Jia, Z.; Ierapetritou, M.; Georgakis, C. Similarities and differences between the concepts of operability and flexibility: The steady-state case, *AIChE J*., *56*, 702, **2010b**.

Liou, C. W. *The impacts of mixers and buffer tanks on the operational flexibility of water usage and treatment networks*. MS Thesis, Chemical Engineering Department, National Cheng Kung University, Taiwan, **2006**.

Malcom, A.; Polan, J.; Zhang, L.; Ogunnaike, B. A.; Linninger, A. A. Integrating systems design and control using dynamic flexibility analysis, *AIChE J*., *53*, 2048, **2007**.

Meindersma, G. W.; Guijt, C. M.; de Haan, A. B. Desalination and water recycling by air gap membrane distillation. *Desalination*., *187*, 291, **2006**.

Mohideen, M. J.; Perkins, J. D.; Pistikopoulos, E. N. Optimal design dynamic systems under uncertainty. *AIChE J.*, *42*, 2251, **1996**.

Ostrovski, G. M.; Achenie, L. E. K.; Wang, Y. P.; Volin, Y. M. A new algorithm for computing process flexibility. *Comput. Chem. Eng.*, *39*, 2368, **2001**.

Ostrovski, G. M.; Volin, Y. M. Flexibility analysis of chemical process: Selected global optimization sub–problems. *Optim. Eng.*, *3*, 31, **2002**.

Petracci, N. C.; Hoch, P. M.; Cliche, A. M. Flexibility analysis of an ethylene plant. *Comput. Chem. Eng.*, *20*, S443, **1996**.

Pistikopoulos, E. N.; Grossmann, I. E. Evaluation and redesign for improving flexibility in linear systems with infeasible nominal conditions. *Comput. Chem. Eng.*, *12*, 841, **1988a**.

Pistikopoulos, E. N.; Grossmann, I. E. Optimal retrofit design for improving process flexibility in linear systems. *Comput. Chem. Eng.*, *12*, 719, **1988b**.

Pistikopoulos, E. N.; Grossmann, I. E. Optimal retrofit design for improving process flexibility in nonlinear systems–I: Fixed degree of flexibility. *Comput. Chem. Eng.*, *13*, 1003, **1989a**.

Pistikopoulos, E. N.; Grossmann, I. E. Optimal retrofit design for improving process flexibility in nonlinear systems–II: Optimal level of flexibility. *Comput. Chem. Eng.*, *13*, 1087, **1989b**.

Quan, J. R.; Chang, C. T. New insights in solving distributed system equations by the quadrature methods— I. *Comput. Chem. Eng.*, *13*, 779, **1989a**. Q15

Quan, J. R.; Chang, C. T. New insights in solving distributed system equations by the quadrature methods— II. *Comput. Chem. Eng.*, *13*, 1017, **1989b**. Q15

Riyanto, E.; Chang, C. T. A Heuristic revamp strategy to improve operational flexibility of water networks based on active constraints, *Chem. Eng. Sci.*, 65, 2758, **2010**.

Shu, C. *Differential Quadrature and Its Applications in Engineering*. London: Springer-Verlag, 340, **2000**.

Soroush, M.; Kravaris, C. Optimal design and operation of batch reactors. 1. Theoretical framework. *Ind. Eng. Chem. Res.*, *32*, 866, **1993a**. Q16

Soroush, M.; Kravaris, C. Optimal design and operation of batch reactors. 2. A case study. *Ind. Eng. Chem. Res.*, *32*, 882, **1993b**. Q16

Swaney, R. E.; Grossmann, I. E. An index for operational flexibility in chemical process design. Part I: Formulation and theory. *AIChE J.*, *31*, 621, **1985a**. Q17

Swaney, R. E.; Grossmann, I. E. An index for operational flexibility in chemical process design. Part II: Computational algorithms. *AIChE J.*, *31*, 631, **1985b**. Q17

Varvarezos, D. K.; Grossmann, I. E.; Biegler, L. T. A sensitivity based approach for flexibility analysis and design of linear process systems. *Comput. Chem. Eng.*, *19*, 1301, **1995**.

Volin, Y. M.; Ostrovski, G. M. Flexibility analysis of complex technical systems under uncertainty. *Automat. Rem. Control*, *63*, 1123, **2002**.

Walsh, S.; Perkins, J. D. Application of integrated process and control system design to waste water neutralization. *Comput. Chem. Eng.*, *18*, S183, **1994**.

White, V.; Perkins, J. D.; Espie, D. M. Switchability analysis. *Comput. Chem. Eng.*, *20*, 469, **1996**.

Zhou, H.; Li, X. X.; Qian,Y.; Chen, Y.; Kraslawski, A. Optimizing the initial conditions to improve the dynamic flexibility of batch processes, *Ind. Eng. Chem. Res.*, *48*, 6321, **2009**.

Zong, Z.; Lam, K. Y. A Localized differential quadrature method and its application to the 2D wave equation. *Comput. Mech.*, *29*, 382, **2002**.

Zong, Z.; Zhang, Y. Y. Advanced *Differential Quadrature Methods*. Boca Raton, FL: Chapman & Hall/CRC, **2009**. Q18

Cat#: K23873 **Chapter: 0010**

TO: CORRESPONDING AUTHOR

AUTHOR QUERIES – TO BE ANSWERED BY THE AUTHOR

The following queries have arisen during the typesetting of your manuscript. Please answer these queries by marking the required corrections at the appropriate point in the text.

Query No.	Query	Response
Q1	Swaney and Grossmann (1983a) is not under References. Please provide complete publication details.	
Q2	Please check rewording of previous sentence did not alter your intended meaning in the sentence 'As mentioned before… .'	
Q3	Variables are inconsistent throughout the chapter, some are in italic and some are bold roman. Please confirm the correct style .	
Q4	All Greek variable should be in roman only. Please check bold θ, λ, μ, ν, ψ.	
Q5	Is it Malcom et al. (2007) or Malcolm et al. (2007)? Please confirm the correct spelling.	
Q6	Is it White et al. (1996) or White et al. (1994)? Please confirm the correct year	
Q7	Please check that rewording did not alter intended meaning in the sentence 'Finally, in the case… .	
Q8	Please check rewording did not alter intended meaning	

	in the sentence ‘This is because… .’	
Q9	Please review that rewording did not alter intended meaning in the sentence ‘When $\phi_{util} < 1$....”	
Q10	Please provide further details in Ref. Burgess and Lovegrove, 2005.	
Q11	Please confirm Chacon–Mondragon and Himmelblau (1996) changed to Chacon-Mondragon and Himmelblau (1996) OK intext and reference list	
Q12	Please confirm the insertion of “a” “b” for Lima et al. (2010) in reference list.	
Q13	Please confirm the insertion of “a” “b” for Pistikopoulos and Grossmann (1988) in reference list.	
Q14	Please confirm the insertion of “a” “b” for Pistikopoulos and Grossmann (1989) in reference list.	
Q15	Please confirm the insertion of “a” :b” for Quan and Chang (1989) in reference list	
Q16	Please confirm the insertion of “a” “b” for Soroush and Kravaris (1993) in reference list.	
Q17	Please confirm the insertion of “a” “b” for Swaney and Grossmann (1985) in reference list.	
Q18	Please check [36] in Table 10.2.	
Q19	Please check Biegler et al. (1987) is not in reference list	